Facile Tandem Copolymerization of *O*-Carboxyanhydrides and Epoxides to Synthesize Functionalized Poly(ester-*b*-carbonates)

Xiaoqian Wang, Rong Tong *

Department of Chemical Engineering, Virginia Polytechnic Institute and State University, 635 Prices Fork Road, Blacksburg, Virginia, 24061, United States.

ABSTRACT: The synthesis of well-defined degradable block copolymers from mixtures of monomers is one of the foremost challenges in the sustainable plastics industry. For example, the currently available one-pot strategies for preparing poly(ester-*co*-carbonates)—which combine two commonly used degradable polymers—are energy- and material-intensive, requiring high-pressure CO_2 gas and elevated temperatures. Here we report an atom-economical, scalable method for block copolymerization of *O*-carboxyanhydrides and epoxides to prepare functionalized poly(ester-*b*-carbonates) with high molecular weights (>200 kDa) and narrow molecular-weight distributions ($Đ < 1.1$) by using a single Lewis acidic zinc complex at room temperature in the absence of pressurized CO_2. Kinetic studies showed that the first stage of the process, ring-opening polymerization of the *O*-carboxyanhydrides, exhibited zero-order kinetics, suggesting that the polymerization rate was independent of monomer concentration and thus allowing for a sharp switch in mechanism without tapering effect. The obtained degradable poly(ester-*b*-carbonates) showed better toughness than their corresponding homopolymers and outperformed some commodity polyolefins.

INTRODUCTION

The synthesis of sequence-defined copolymers, such as block copolymers, enables the material properties of the constituent homopolymers to be combined in single copolymers with new sets of features.[1] However, synthesizing sequence-defined copolymers from monomer mixtures is widely regarded as one of the paramount challenges in polymer chemistry.[2] Traditional strategies for polymerizing two mechanistically incompatible monomers into a single block copolymer involve using bifunctional initiators[3] or catalysts[4] or changing the active species upon formation of the first block[5] (Figure 1a). Recently, the emergence of switchable / tandem polymerization strategies in which a single catalyst is used to access and switch between catalytic cycles of ring-opening polymerization (ROP) and ring-opening copolymerization (ROCOP) has opened a realm of auto-tandem catalysis processes for preparing sequence-controlled block copolymers (Figure 1b).[6] The copolymer sequences generated in this way can be precisely controlled by external stimuli, such as changes in gas pressure,[7] changes in redox state,[8] and electricity.[9] Such strategies have been used for switchable polymerization chemistry focusing on the preparation of poly(ester-*co*-carbonates) from various combinations of renewable monomers including lactones, anhydrides, epoxides, and CO_2.[10] By combining the properties of their respective homopolymers, the obtained aliphatic poly(ester-*co*-carbonates) show improved thermal and mechanical properties relative to those of the homopolymers.[11] Nevertheless, the currently available methods for switchable polymerization reactions involving organometallic catalysts are energy-intensive: the reactions often require elevated temperature (50–120 °C) and high CO_2 pressure (5–20 bar).[7,10-11] Switchable / tandem polymerization reactions involving organocatalysts, such as bifunctional organoborons[12] and Lewis pairs,[13] also require high temperature (50–100 °C) and pressurized CO_2 (~10 bar) and provide copolymers that have molecular weights (MWs) of less than 100 kDa and broad MW distributions ($Đ > 1.2$). Finally, the monomers that have been used for switchable / tandem polymerization have a restricted functionality window—most of the monomers have no functionality other than simple pendant alkyl side chains. Therefore, the search for milder, more energy-efficient methods for controlled tandem polymerization to afford high-MW functionalized poly(ester-*co*-carbonates) is ongoing.

Among the monomers most commonly explored for the synthesis of functionalized polyesters are *O*-carboxyanhydrides (OCAs) with pendant functional groups. These compounds, which are prepared from renewable resources (amino or hydroxy acids), are highly active and afford readily diversifiable polymers.[14] We recently reported the use of OCAs for stereoselective synthesis of high-MW polyesters (>200 kDa) that exhibit better ductility and toughness than commodity low-density polyethylene (LDPE).[15] The incorporation of functional-group-bearing OCAs into switchable polymerization reactions has been explored. For example, the Williams group recently reported ground-breaking work showing that OCAs and epoxides can be copolymerized by a dinuclear Zn complex (Figure 1c).[16] In these reactions, the CO_2 molecule released from ROP of the OCA is recycled into a ROCOP reaction between the epoxide and CO_2 to produce poly(ester-*b*-carbonates) (*b*, block) with high atom economy. Similarly, switchable polymerization has also been achieved with organocatalysts.[17] Notably, the dinuclear-Zn-complex-catalyzed copolymerizations reported by Williams et al. require a high temperature (80 °C), whereas the same reactions involving organocatalysts can be carried out at room temperature. However, both of these one-pot methods for the tandem copolymerization give polymers with low MWs (< 20 kDa) and relatively broad MW distributions ($Đ \sim 1.2$), and excess epoxide is required. Thus far, a facile method for preparing high-MW functionalized poly(ester-*b*-carbonates) has not been achieved, and

the lack of such a method limits access to these degradable block copolymers, which show promising thermal and mechanical properties.

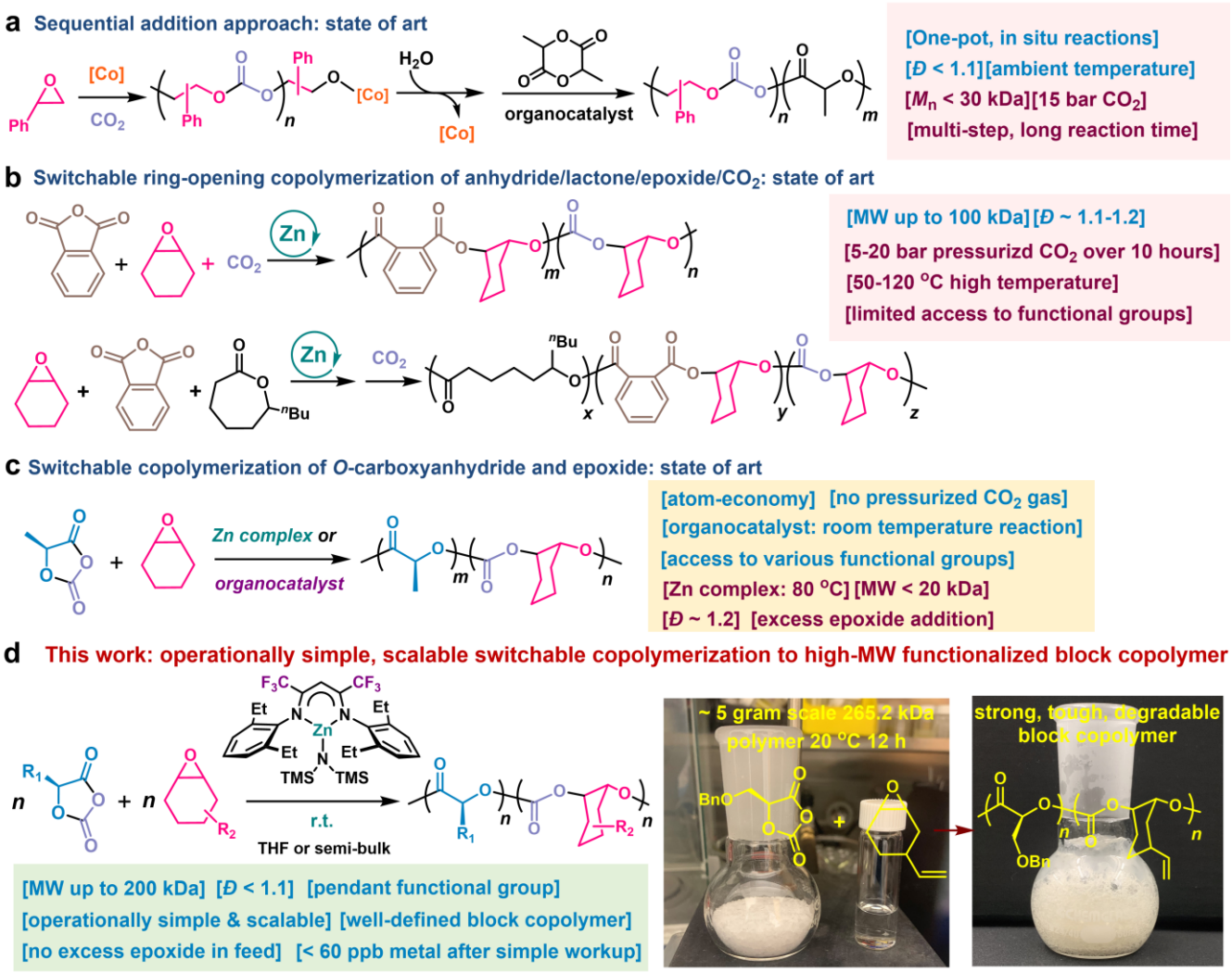

Figure 1. Strategies for synthesis of high-molecular-weight (MW) functionalized poly(ester-*b*-carbonates). (a) Synthesis of block copolymers by sequential addition of epoxides/CO_2 and lactides. (b) Mechanism-switchable anhydride/epoxide/lactone/CO_2 ring-opening copolymerization with catalysis by a single metal complex. (c) Mechanism-switchable *O*-carboxyanhydride (OCA)/epoxide polymerization to afford low-MW copolymers with broad MW distributions. (d) Scalable tandem OCA/epoxide copolymerization at room temperature to afford high-MW functionalized block copolymers, as reported in this paper. The pros and cons of the various strategies are indicated in blue and red type, respectively.

In this study, we identified a Zn complex that mediates strikingly selective one-pot tandem polymerizations of OCAs and epoxides at room temperature to afford high-MW (>200 kDa) functionalized poly(ester-*b*-carbonates) with narrow MW distributions ($Đ$ < 1.1), using a remarkably simple and scalable experimental setup (Figure 1d). Our mechanistic studies uncover unusual zero-order kinetics that provides a unique strategy for achieving precise sequence control in a mixture of co-monomers. The obtained copolymers have high tensile stress (fracture stress > 20 MPa) and excellent ductilities (fracture strain > 400%), outperforming commodity polyolefins such as LDPE and polypropylene. The copolymers can be sequentially and efficiently degraded to the corresponding monomers for recycling.

RESULTS AND DISCUSSION

Identification of Conditions for Zn-Mediated Tandem Copolymerization. We began by studying (BDI)Zn complexes (BDI = β-diiminate) as catalysts for OCA/epoxide copolymerization. These versatile complexes have been used for stereoselective ROP of lactones[18] and OCAs[19] and can also mediate epoxide/CO_2 ROCOP[20] and epoxide/anhydride ROCOP.[21] We initially focused on the copolymerization of cyclohexene oxide (CHO) and OCA **2** mediated by various (BDI)Zn complexes at room temperature in THF ([**2**]/[CHO]/[Zn] = 100/100/1; Figure 2a). Much to our dismay, catalysts **Zn-4** and **Zn-5**, which have an electron-withdrawing cyano group and are active for CHO/CO_2 and CHO/anhydride copolymerization,[21-22] did not initiate CHO/CO_2 copolymerization after the **2** was consumed. Previous studies of ROCOP catalysts demonstrated that increasing the Lewis acidity of a catalyst by changing the ligand structure improves epoxide activa-

tion.[23] Indeed, we found that **Zn-7**, which has two electron-withdrawing CF_3 groups in the BDI ligand backbone,[24] mediated **2**/CHO copolymerization at room temperature, resulting in 100% OCA conversion and 90% CHO conversion after 12 h. The obtained copolymer had a M_n of 29.9 kDa and a $Đ$ of 1.01 (expected MW = 32.0 kDa). We reasoned that the **Zn-7** outperformed **Zn-4** and **Zn-5** because the electron-withdrawing CF_3 group has a higher value of electronegativity of 3.49 (Pauling scale) compared with the CN group

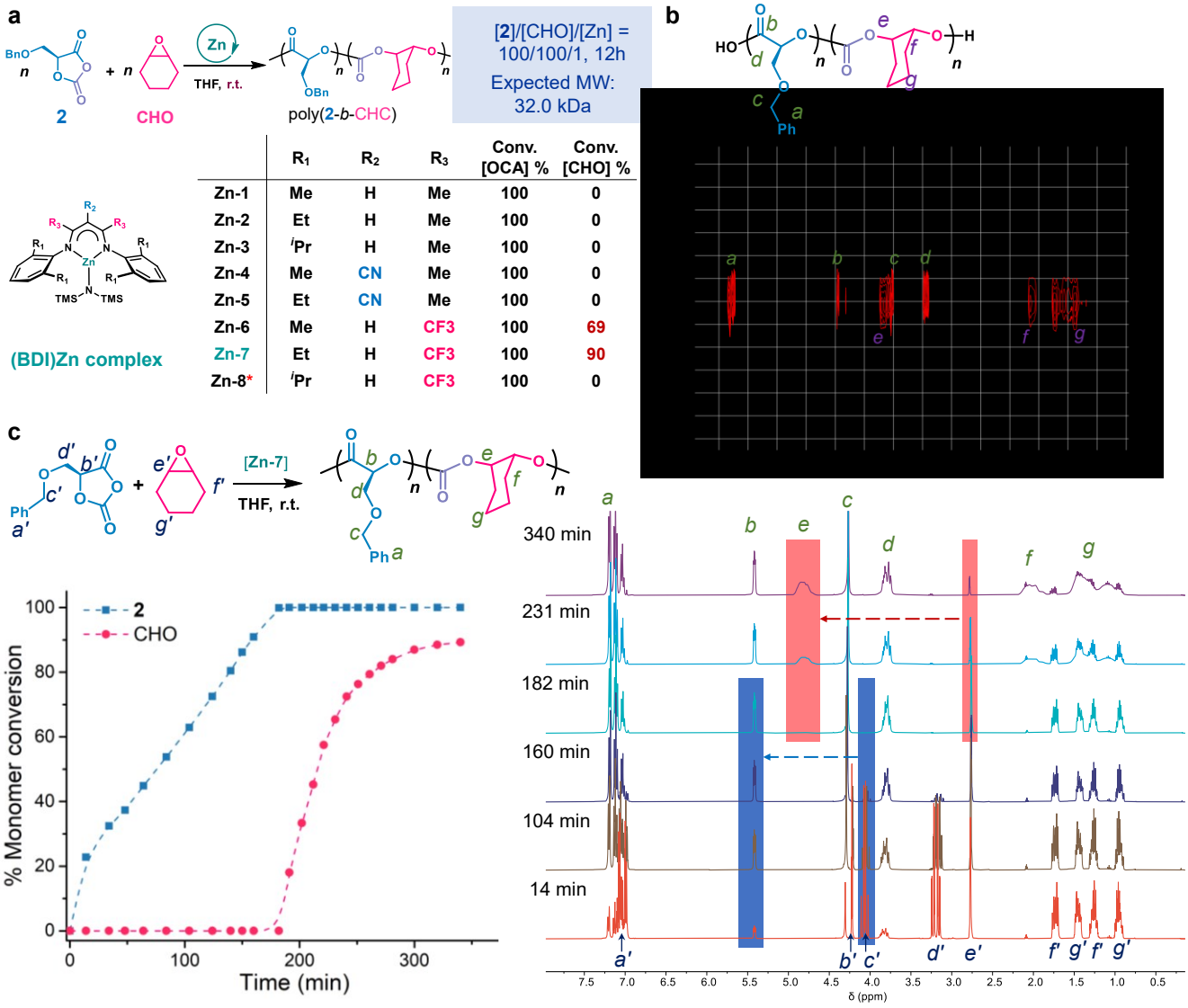

	R_1	R_2	R_3	Conv. [OCA] %	Conv. [CHO] %
Zn-1	Me	H	Me	100	0
Zn-2	Et	H	Me	100	0
Zn-3	^{i}Pr	H	Me	100	0
Zn-4	Me	CN	Me	100	0
Zn-5	Et	CN	Me	100	0
Zn-6	Me	H	CF3	100	69
Zn-7	Et	H	CF3	100	90
Zn-8*	^{i}Pr	H	CF3	100	0

Figure 2. Zn-mediated block copolymerization of *O*-carboxyanhydride **2** and cyclohexene oxide (CHO). (a) Identification of the reactive **Zn-7** complex that enabled efficient **2**/CHO copolymerization at room temperature with high monomer conversion. Detailed polymerization data are provided in Table S2. *, **Zn-8** had the initiating group of -Et instead of -N(TMS)$_2$. (b) Diffusion-ordered (DOSY) NMR spectrum of poly(**2**-*b*-CHC) (^{1}H, ^{13}C, and two-homopolymer-mixture DOSY NMR spectra are shown in Figures S1 and S3). (c) Representative kinetics data for monomer conversion as determined by real-time ^{1}H NMR spectroscopy. The peak shifts due to conversion of **2** to the poly(**2**) block and conversion of CHO to the poly(CHC) block are highlighted in blue and red, respectively.

(2.77).[25] The substituent on the *N*-aryl group of the (BDI)Zn complex also affected the polymerization outcome (compare the results for **Zn-7** with those for **Zn-6** and **Zn-8** in Figure 2a). Screening of other metal complexes that have been used to catalyze polyester and polycarbonate synthesis did not yield results comparable to those obtained with **Zn-7** (Table S1), and neither did Zn complexes with tridentate ligands (Table S2). Notably, the Rieger group reported that epoxide/CO_2 ROCOP mediated by the Lewis acidic **Zn-7** complex requires a relatively high temperature (50 °C) and pressurized CO_2 (40 bar);[23b] whereas we found that **Zn-7**-mediated ROCOP of CHO/CO_2 could be conveniently achieved at room temperature with 1 bar CO_2 to afford a poly(cyclohexene

carbonate) (poly(CHC)) with a M_n of 42.9 kDa and a $Đ$ of 1.06 (Table S3, entry 2).

We then determined whether the copolymerization afforded a random copolymer, a mixture of two homopolymers, or a block copolymer. A DOSY NMR study (DOSY = diffusion-ordered spectroscopy) of the obtained polymer showed a single diffusion coefficient for all resonances, as would be expected for a copolymer (Figure 2b); whereas the DOSY NMR spectrum of a physical mixture of poly(**2**) and poly(CHC) homopolymers showed two diffusion coefficients (Figure S1). To determine whether the two monomers were incorporated randomly or into a well-defined block copolymer, we monitored the **Zn-7**-mediated copolymerization in deuterated toluene by means of real-time ^{1}H NMR spectroscopy (Figure 2c). Note that Fourier transform IR spectroscopy was unsuitable for elucidating the kinetics because the epoxide IR peaks (the stretch peak at ~1239 cm^{-1} and the peak at ~1176 cm^{-1})[6c] were interfered with by neighboring peaks (Figure S2). The typical NMR spectra shown in Figure 2c clearly demonstrate that the polymerization occurred in two stages: in the first stage, ROP of **2** proceeded with release of CO_2 to form poly(**2**) block; and, in the

Table 1. Copolymerization of Epoxides and *O*-Carboxyanhydrides at Room Temperature.[a]

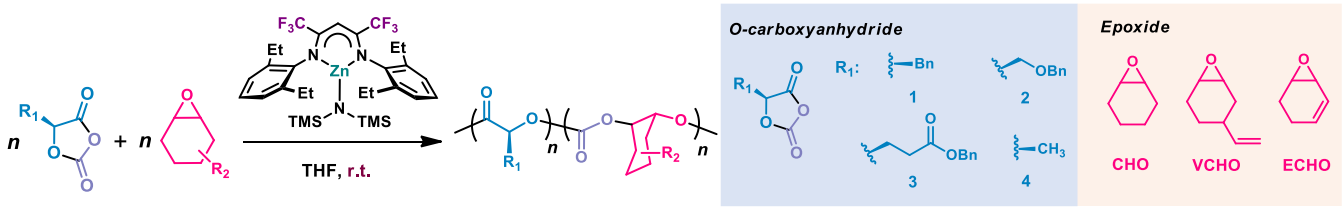

Entry	OCA/epoxide	FR	Time (h)	OCA conv. (%) [b]	Epoxide conv. (%) [c]	Co-polymer yield (%)	M_n (kDa) [d]	MW_{cal} (kDa)	$Đ$ [d]
1	**2**/CHO	300/300	4	100	89.5	95.3	77.6	91.6	1.01
2	**2**/CHO [e]	300/300	4	100	72.5	87.8	88.1	84.3	1.03
3 [f]	**1**/CHO	300/300	2	100	63.0	81.9	60.4	71.3	1.01
4	**3**/CHO	300/300	12	100	89.5	95.8	92.5	104.2	1.01
5	**4**/CHO	300/300	1	100	100	100	71.3	64.2	1.05
6	**1**/VCHO	300/300	12	100	87.0	93.1	101.7	88.3	1.01
7	**2**/VCHO	300/300	12	100	100	100	177.6	103.8	1.01
8	**2**/VCHO	600/600	12	100	100	100	265.4	207.7	1.01
9	**3**/VCHO	300/300	24	100	100	100	141.3	116.5	1.02
10	**4**/VCHO	300/300	12	100	100	100	79.2	72.3	1.03
11	**2**/ECHO	100/100	12	100	100	100	20.0	31.8	1.04
12	**2**/CHO/VCHO [g]	300/150/150	12	100	100/ 100	100	90.2	99.9	1.01
13	**4**/VCHO + **2**/CHO [h]	300/300 + 300/300	12 + 12	100/ 100	100/ 73.5	93.3	155.1 (79.2)	157.0 (72.3)	1.09 (1.03)

[a] Abbreviations: OCA, *O*-carboxyanhydride; FR, [OCA]/[**Zn-7**] feed ratio; Conv., conversion; M_n, number-average molecular weight; MW_{cal}, molecular weight calculated from FR and monomer conversion; $Đ$, molecular weight distribution; CHO, cyclohexene oxide; VCHO, vinyl cyclohexene oxide; ECHO, 3,4-epoxy-1-cyclohexene; CHC, cyclohexene carbonate. Polymerization conditions: [OCA] = [epoxide] = 2.0 M in THF at room temperature in a glove box. [b] Determined from the intensity of the Fourier transform IR peak at 1805 cm^{-1}, which corresponds to the anhydride group of the OCA. [c] Determined by ^{1}H NMR spectroscopy. [d] Determined by SEC. [e] THF (10 μL) was used to dissolve **Zn-7** (0.53 μmol) for this semibulk polymerization. n(**2**) = n(CHO) = 0.159 mmol. [f] The poly(CHC)/cyclic CHC ratio was 0.926/0.074 at the end of copolymerization, as measured by

^{1}H NMR spectroscopy (see Figure S9). [g] CHO and VCHO were mixed together ([CHO] = [VCHO]) with **2** for the copolymerization. [h] An **2**/CHO mixture was added to the reaction mixture after formation of the first diblock copolymer was complete, as confirmed by ^{1}H NMR spectroscopy (see SI section S3.2). The numbers in parenthesis in the M_n and $Đ$ columns are SEC results for the first diblock, i.e., poly(**4**-*b*-VCHC).

second stage, ROCOP of CHO and the CO_2 released by the ring-opening of **2** afforded a poly(CHC) block (poly(CHC) block formation started at ~182 min), confirming the formation of a sequence-defined block copolymer. Notably, these NMR studies also suggested that no polyether side products (~3.46 ppm) formed during the polymerization. Carbonate bond formation was confirmed from the ^{13}C NMR spectrum of the obtained block copolymer (153.9 ppm), and such NMR spectrum also suggested isoselective enchainment of the poly(CHC) block with a high probability of meso dyad formation (P_m = 0.85, Figure S3b).[26] The obtained block copolymer exhibited narrow unimodal MW distribution, determined by size-exclusion chromatography (SEC, Figure S3c-d). We note that the matrix-assisted laser desorption/ionization mass spectrum (MALDI-MS) of the oligomer ([**2**]/[CHO]/[**Zn-7**] = 5/5/1; Figure S4a) also indicated the block copolymer formation.

The discovery of **Zn-7**-mediated auto-tandem block copolymerization of **2** and CHO prompted us to optimize the reaction conditions. Examination of the initiating group on **Zn-7** revealed that a complex with a bis(trimethylsilyl)amido group gave the best results (Table S4, entry 1); Zn complexes bearing an ethyl, methyl lactate, or acetate group did not adequately incorporate CHO into the copolymer (entries 2–4). Surprisingly, the addition of BnOH into the reaction mixture did not efficiently enchain the CHO/CO_2 ROCOP in the copolymerization (entry 5), suggesting that the Zn-alkoxide might not be efficiently converted to a Zn-carbonate to initiate CHO/CO_2 copolymerization(see below mechanistic studies). The presence of CHO was essential to the ROP of OCA in the copolymerization (Table S3, entry 3). Although lowering the reaction temperature slowed the first stage (ROP of OCA, entry 5), increasing the temperature reduced the amount of CO_2 dissolved in the reaction mixture (entry 6). Externally applying CO_2 with a gauge pressure of 1 bar during the second stage (CHO/CO_2 ROCOP) had a negligible effect on the MW (entry 7), indicating that the soluble CO_2 liberated from **2** was sufficient.

Next we investigated whether our method could afford copolymers with MWs predictable from the initial monomer/catalyst feed ratio. We found that the M_n values of the copolymers increased linearly as the [**2**]/[CHO]/[**Zn-7**] feed ratio was increased from 50/50/1 to 300/300/1, and all the obtained copolymers had $Đ$ values of <1.1 (Figure 3a; SEC traces of the copolymers are shown in Figure S5). At the highest [**2**]/[CHO]/[**Zn-7**] ratio (300/300/1), the conversion of **2** was quantitative, and CHO conversion reached 89.5% in 4 hours (Table 1, entry 1). Note that no epimerization of the α-methine hydrogen was observed in the ^{1}H or ^{13}C NMR spectrum of the poly(**2**) block of high-MW poly(**2**-*b*-CHC) (Figure S3a, b). Importantly, the copolymerization could be conducted on a multigram scale under semibulk conditions in neat CHO (liquid, [CHO]/[**2**]/[**Zn-7**] = 300/300/1) containing a trace of THF (10 μL) to dissolve the **Zn-7**; under these conditions, we obtained a copolymer with M_n and $Đ$ values comparable to those of the copolymer obtained from a solution-phase reaction (compare entries 1 and 2 in Table 1). Inductively coupled plasma mass spectrometry (ICP-MS) revealed that a negligible amount of Zn ([Zn] < 60 ppb) remained in the copolymer after the dichloromethane solution of the copolymer was added to cold methanol to precipitate the copolymer (Table S5).

Copolymerization Scope and Multiblock Copolymerization. With an optimized set of conditions in hand, we examined the copolymerization of OCAs **1**–**4** with CHO at room temperature. The reaction with **3** for 12 h gave a M_n of 92.5 kDa (Table 1, entries 3–5). The $Đ$ values of all the obtained polymers were less than 1.1 (SEC traces are shown in Figures S6–S8), suggesting that side reactions did not occur.[27] Notably, a cyclic carbonate of CHO formed in an overnight reaction of L-**1** with CHO (see the ^{1}H NMR kinetic studies in Figure S9), but this compound was not detected in reactions involving other OCA/CHO combinations (see the NMR spectra in Figures S6–S8). In addition, we explored the copolymerization of OCAs **1**–**4** with two other epoxides: vinyl cyclohexene oxide (VCHO) and 3,4-epoxy-1-cyclohexene (ECHO, Table 1, entries 6–11). Both copolymerizations were achieved with high monomer conversions and gave products with low $Đ$ values (<1.1), and ^{1}H NMR spectroscopy showed no evidence of ether linkages or cyclic carbonates (Figures S10–S14). Notably, copolymerization with VCHO allowed for the preparation of a functionalized high-MW copolymer with a M_n of 265.4 kDa and a $Đ$ of 1.01 ([**2**]/[VCHO]/[**Zn-7**] = 600/600/1; Table 1, entry 8). The versatility of **Zn-7** was also apparent in the **2**/CHO/VCHO terpolymerization, which proceeded with high conversion of all the monomers (entry 12) without undesired polyether formation (Figure S15). Nevertheless, we note that **Zn-7** displayed lower reactivity toward alkylene oxides (e.g. propylene oxide; epoxide conversion < 10%) compared to CHO derivatives in both ROCOP of epoxide/CO_2 and the copolymerization of OCA/epoxide, behavior that is similar to that of many Zn complexes in the epoxide/CO_2 ROCOP.[28] Finally, we determined whether multiblock copolymers could be prepared in one pot by sequential addition of the OCA/epoxide monomer combinations, e.g., **4**/VCHO followed by **2**/CHO (entry 13). In this way, tetrablock copolymer poly(**4**-*b*-VCHC-*b*-**2**-*b*-CHC; VCHC = vinyl cyclohexene carbonate) could be readily synthesized with quantitative monomer conversion and remarkable control of M_n and $Đ$ (SEC traces are shown in Figure S16), indicating the living nature of our copolymerization with an active chain-end.

Polymerization Kinetics and Mechanistic Studies. We used ^{1}H NMR spectroscopy to profile the kinetics of [**2**]/[CHO] copolymerization at various **Zn-7** concentrations ([**2**] = [CHO] =

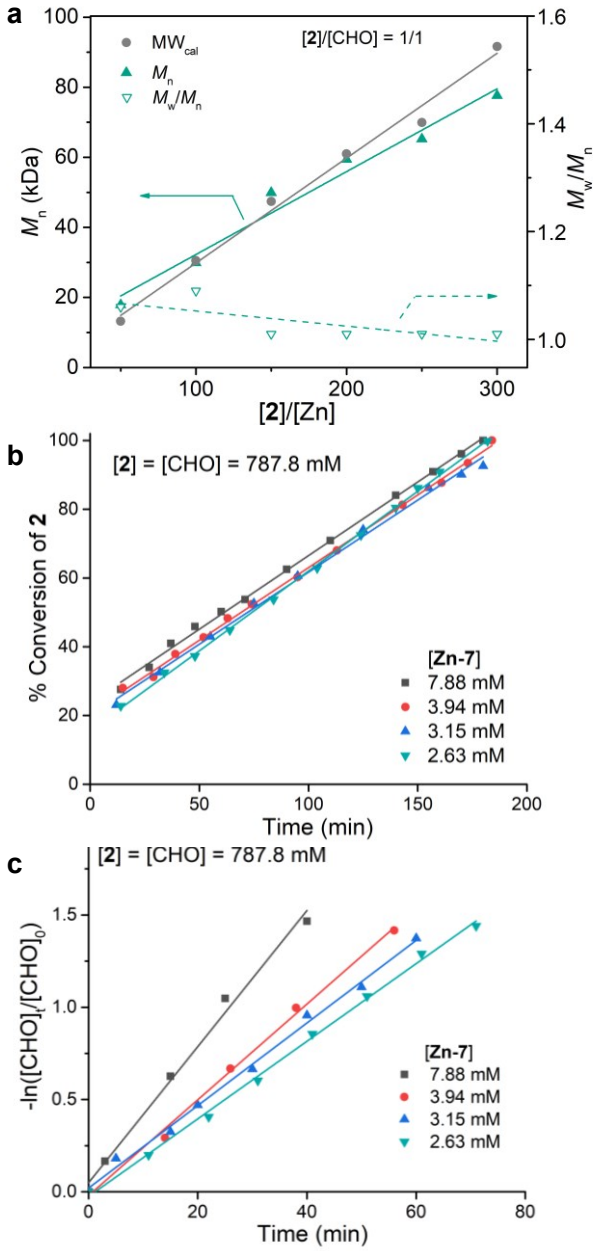

Figure 3. Controlled living copolymerization of *O*-carboxyanhydride **2** and cyclohexene oxide (CHO). (a) Plots of M_n and MW distribution (M_w/M_n) versus [**2**]/[**Zn-7**] feed ratio at room temperature. (b) Plots of **2** conversion versus time at various **Zn-7** concentrations in the polymerization of the poly(**2**) block of poly(**2**-*b*-CHC). (c) Plots of CHO conversion versus time at various **Zn-7** concentrations in the polymerization of the poly(CHC) block of poly(**2**-*b*-CHC).

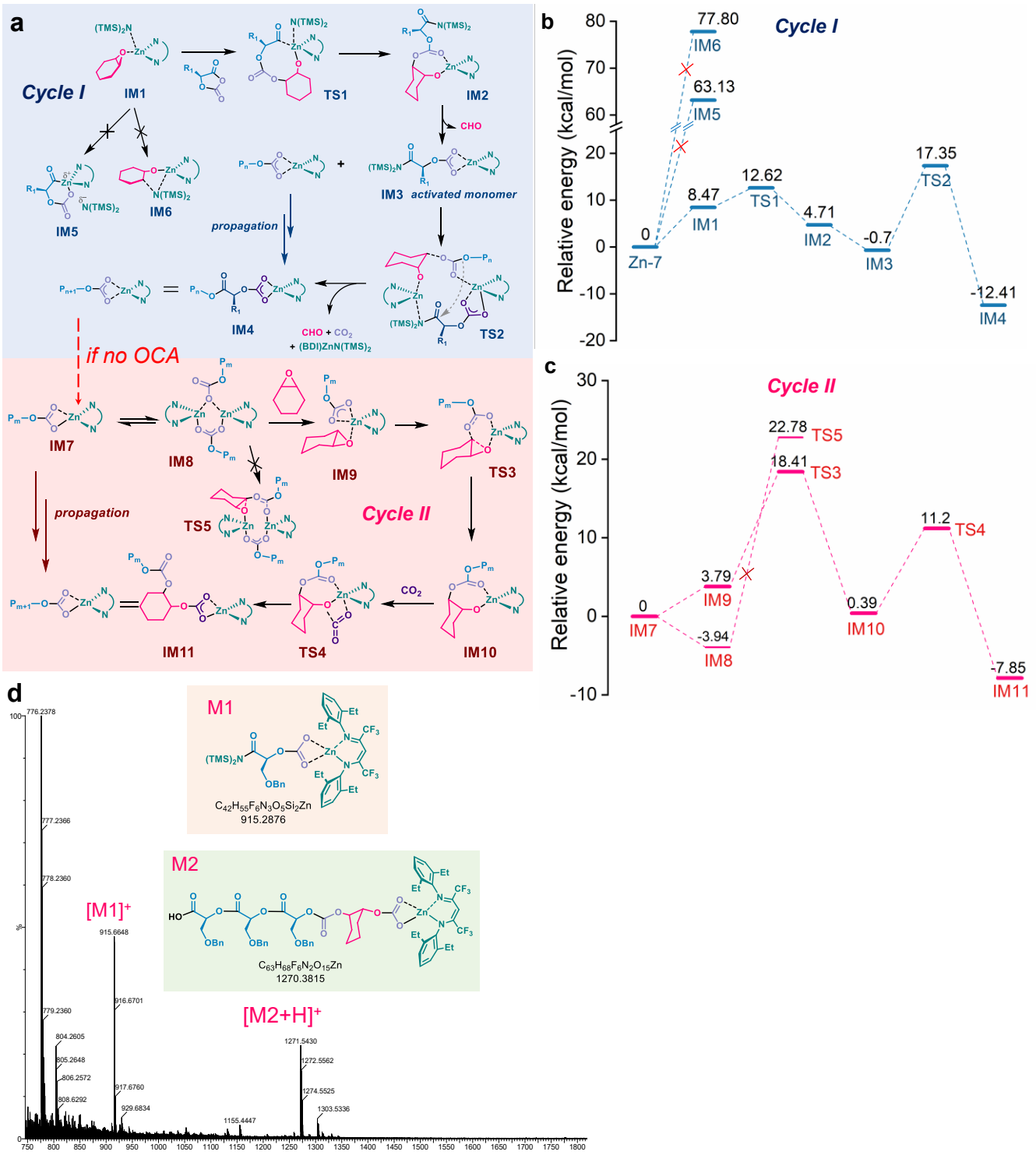

Figure 4. Proposed mechanism for auto-tandem block copolymerization of *O*-carboxyanhydride / epoxide with supporting evidence. (a) Proposed copolymerization mechanism that switches from *O*-carboxyanhydride ring-opening polymerization (ROP, cycle I) to epoxide/CO_2 ring-opening copolymerization (ROCOP, cycle II). The proposed mechanism was supported by the free energies of (b) ROP in cycle I and (c) ROCOP in cycle II calculated by means of density functional theory. Detailed three-dimensional structures of optimized intermediate states are shown in Figures S21-S22, and SI section S7. (d) Electrospray ionization mass spectrometry of the reaction of [**2**]/[CHO]/[**Zn-7**] (3/3/1), in support of the pathway shown in (a). Detailed peak assignments and mechanism pathway discussions are provided in Figure S19.

787.8 mM in deuterated toluene). Surprisingly, the rate of **2** consumption during ROP of OCA clearly showed a strict zero-order dependence on **Zn-7** concentration, with no induction period at any of the tested **Zn-7** concentrations (Figure 3b). When the individual monomer concentrations were varied, double logarithm plots of apparent first-stage polymerization rate constant (k_{app}) versus monomer concentration gave reaction orders of 2.05 ± 0.18

and −1.99 ± 0.12 for CHO and **2**, respectively (Figure S17a–d). Thus, the first stage, ROP of **2**, exhibited the following rate law:

$$-d[\mathbf{2}]/dt = k_{p1}[CHO]^{2.05}/[\mathbf{2}]^{1.99} \quad (1)$$

where k_{p1} is the propagation rate constant of the first stage ROP of OCA. When equal amounts of CHO and **2** were used and experimental errors are considered, the rate law becomes

$$-d[\mathbf{2}]/dt = k_{p1} \quad (2)$$

as presented in Figure 3b.

Additionally, investigation of the rate of ROCOP of CHO and CO_2 liberated from **2** revealed a reaction order of 0.52 ± 0.05 with respect to **Zn-7** concentration, a first-order dependence on [CHO], and no dependence on the concentration of **2**, which was the CO_2 source (Figure 3c; Figure S17e, f). Since **Zn-7** is monomeric in crystal form,[29] the reaction order of **Zn-7** suggested that the Zn complex at the poly(CHC) chain-end likely participated in a monomeric transition state (cycle II in Figure 4a, c; see discussion in Figure S17).[30] The independence of poly(CHC) enchainment with respect to the concentration of **2** (the CO_2 source, Figure S17f) agrees well with previously reported rate laws for BDI-Zn-mediated CHO/CO_2 copolymerization.[30] Therefore, the second stage, **Zn-7**-mediated copolymerization of CHO and CO_2, showed the following rate law:

$$-d[CHO]/dt = k_{p2}[CHO]^{1}[\mathbf{Zn\text{-}7}]^{0.52} \quad (3)$$

where k_{p2} is the propagation rate constant of the second stage ROCOP of CHO/CO_2.

The zero-order dependence of the rate on catalyst concentration, the inverse order dependence on monomer concentration, and the dispensability of an alcohol initiator (Figure 3b; Figure S17) in the ROP of **2** seem counterintuitive because the rates of most controlled ROPs of OCAs mediated by metal-alkoxide initiators exhibit first-order dependence on monomer concentration and positive reaction orders with respect to catalyst concentration.[15,19] However, zero-order polymerization rates have been observed sporadically for other tandem anhydride/epoxide/CO_2[6a] or anhydride/epoxide/lactone[6c,31] polymerizations. Interestingly, in one switchable anhydride/CHO/lactone polymerization,[6c] even lactone homopolymerization was significantly faster than the zero-order anhydride/CHO ROCOP; anhydride/CHO copolymerization occurred first, without lactone ROP. In addition to the computationally predicted differences in activation energy for the different polymerization mechanisms,[10] zero-order kinetics may be critical for a clean switch in the polymerization mechanism because chain propagation rate is independent of monomer concentration, allowing for circumvention of chain transfer or undesired mechanism switching due to the tapered reaction rate that is observed for polymerizations with first-order kinetics.[32]

The unusual zero-order dependence of the **2** ROP rate on **Zn-7** concentration motivated us to explore the polymerization mechanism. Notably, we found that the ROP did not occur in the absence of CHO (Table S3, entry 3), and even the ring-opening reaction failed to occur when an equimolar mixture of **2** and **Zn-7** was used (Figure S18c); these results suggest that CHO was indispensable for the copolymerization. Nevertheless, no reactions between **2** and CHO or between **Zn-7** and CHO were observed (Figure S18b, d); the ^{1}H NMR peaks of CHO seemed to remain unchanged during the ROP of OCA (Figure 2c), even in the NMR spectrum of an equimolar **2**/CHO/**Zn-7** mixture (Figure S18a). The MALDI-MS of oligo(**2**-*b*-CHC) suggested that CHO was unlikely to have initiated the ROP (Figure S4). The electrospray ionization mass spectrum (ESI-MS) of the **2**/CHO/**Zn-7** mixture ([**2**]/[CHO]/[**Zn-7**] = 3/3/1) indicated that the Zn-carbonate remained at the chain-end during enchainment (Figure 4d), ruling out the possibility that CHO initiated the ROP of **2**; this behavior was different from that previously proposed for OCA/epoxide copolymerization.[16-17] Given that addition of BnOH resulted in inefficient enchainment in the ROCOP (Table S4, entry 5), and that the Zn-alkoxide-mediated ROP of OCA followed first-order kinetic rates[15,19] that differed from our observed kinetics (Figure 3b), ROP of **2** (the first stage in the copolymerization) disfavored the Zn-alkoxide-mediated pathway. Instead, the Zn-carbonate was likely involved in enchainment during the first-stage (ROP) enchainment. The absence of Zn concentration from the observed rate law (eq. 1) and the inverse reaction order with respect to OCA imply that the mechanism involves a Zn-complex-activated monomer that regulates the chain-end reactivities;[33] and the need for CHO led us to postulate that this Zn-activated monomer might require CHO for the enchainment. Indeed, in the ESI-MS of a **2**/CHO/**Zn-7** mixture and a **3**/CHO/**Zn-7** mixture, we detected silylamide-capped OCA-Zn-carbonate complexes (**M1** in Figure 4d; Figures S19 and S20), supporting the plausibility of the proposed activated-monomer species. Thus, we hypothesize that the first stage (ROP of OCA) proceeds via the monomer-activated mechanism shown in Figure 4a. First, CHO/**Zn-7**-mediated ring-opening of **2** generates Zn-carbonate complex **IM3** as the activated monomer. In the presence of abundant CHO, propagation by means of a bimetallic intermolecular reaction between the activated monomer and the Zn-alkoxide chain (via **TS2**) induces decarboxylation, giving rise to a new Zn-carbonate (**IM4**) upon release of CHO, CO_2, and **Zn-7** (Figure S21).

To evaluate the validity of this mechanistic hypothesis and to gain further insight into reaction pathways, we performed extensive density functional theory (DFT) calculations on a slightly simplified system (i.e., we used **4** instead of **2**) at the SMD_{THF}/wB97M-V/def2-TZVP // SMD_{THF}/B3LYP-D3/6-31G(d)[LANL2DZ(Zn)] level of theory (Figure 4b, c). Note that the direct ring-opening of **4** or CHO by **Zn-7** was predicted to be highly endergonic, with the activation energy barrier of 63.13 kcal/mol (**IM5**) or 77.80 kcal/mol (**IM6**), respectively; whereas the CHO/**Zn-7**-mediated reaction via our proposed activated-monomer mechanism was favored, with a free energy barrier of 4.15 kcal/mol (**IM1** to **TS1**) and a total free energy decrease of 7.77 kcal/mol from **IM1** to the activated monomer (**IM3**, Figure 4b). Additionally, we performed DFT calculations on the second stage (the ROCOP cycle) involving a monomeric Zn-mediated CHO ring-opening followed by CO_2 insertion (Figure 4c; Figure S22). The overall driving force for one second-stage cycle is predicted to be a free energy decrease of 7.85 kcal/mol (Figure 4c). Our calculated energy profiles showed that the dinuclear-Zn-complex-mediated decarboxylation (via **TS2**) and the ring-opening of CHO (via **TS3**) were likely the rate-limiting steps. Additionally, the DFT computation also rationalized the mechanism switching: the calculated energy barrier for OCA ring-opening (**Zn-7** to **TS1**, 12.62 kcal/mol) was much lower than that calculated for CHO-ring-opening (**IM7** to **TS3**, 18.41 kcal/mol). Taken together, these

results indicate that the absence of CO_2 enabled rapid initiation of OCA ROP via the activated-monomer mechanism; the zero-order ROP kinetics ensured that the rate of the first-stage polymerization did not taper before the OCA monomer was consumed; and the computed activation energy barriers for the two polymerizations supported the thermodynamic chain-end preference during the copolymerization, which assured the precise block structure in the obtained copolymer.

Sequential Degradation of Functionalized Poly(ester-*b*-carbonates). Polyesters and polycarbonates can be fully degraded to their respective monomers or monomer derivatives.[15,34] To avoid the difficulty in separating the monomers from each other after poly(ester-*b*-carbonate) degradation, we investigated a sequential degradation strategy for quantitatively recycling the monomers (Figure 5). First, poly(**2**-*b*-CHC) was treated with $Zn[N(TMS)_2]_2$ (10 wt%) in MeOH at 50 °C for 12 h[15] to completely degrade the poly(**2**) block into the corresponding methyl esters, as indicated by ^{1}H NMR spectroscopy (Figure S24). Under these conditions, the poly(CHC) block was insoluble in the reaction mixture and retained its original MW and narrow $Đ$ (Figure S23 and S24g). After the insoluble Zn-alkoxides and polycarbonates were removed from the reaction mixture by centrifugation, dichloromethane was added, the insoluble material was filtered off, and the polycarbonates in the filtrate was treated with 1,5,7-triazabicyclo[4.4.0]dec-5-ene (4 mol%) at 110 °C in toluene for 12 h; this procedure quantitatively yielded the cyclic carbonate monomer, as determined by ^{1}H NMR spectroscopy (Figure S24). Note that the degradation of the poly(VCHC) block of poly(**2**-*b*-VCHC) required a larger amount of 1,5,7-triazabicyclo[4.4.0]dec-5-ene (20 wt%) to fully degrade the polymers into the epoxide monomer (VCHO, Figure S25).

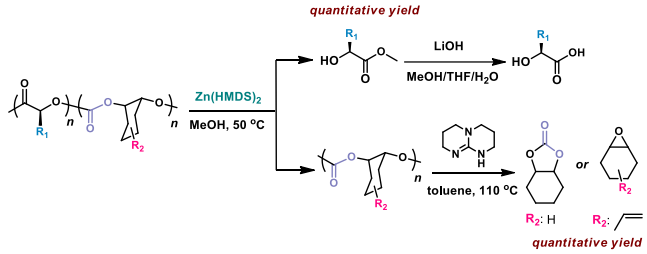

Figure 5. Efficient sequential degradation of poly(ester-*b*-carbonates) to α-hydroxy acids (the precursors of *O*-carboxyanhydrides) and cyclic carbonate or epoxide monomers.

Assessment of Poly(ester-*b*-carbonate) Strength, Ductility, and Toughness. Having developed a scalable method for synthesis of functionalized poly(ester-*b*-carbonates), we turned our attention to assessing their thermal and mechanical properties and exploring their potential applications. Predictably, the mechanical properties of these poly(ester-*b*-carbonates) were affected by their MWs. For instance, high-MW poly(**3**-*b*-CHC) (M_n = 81.5 kDa) exhibited better fracture stress (σ) and toughness than low-MW poly(**3**-*b*-CHC) (M_n = 33.4 kDa) (Figure S26a), highlighting the importance of preparing high-MW copolymers.

The homopolymers poly(CHC), poly(VCHC), and poly(lactic acid) (poly(**4**), PLA) are brittle, with σ values of 25–50 MPa and fracture strain (ε) values of less than 15% (Figure 6a; Table 2, entries 1–3). Although the block copolymers poly(**4**-*b*-CHC) (entry 4), poly(**1**-*b*-CHC), and poly(**1**-*b*-VCHC) (Figure S26b) were also brittle, poly(**4**-*b*-VCHC)—a combination of two brittle polymers—exhibited significantly improved ductility, with an ε of 41.2%, which is 3.6 and 13.3 times the respective values for poly(**4**) and poly(VCHC), with little decrease in the tensile stress (σ = 44.8 MPa, entry 5; Figure 6a). In addition, the tetrablock copolymer poly(**4**-*b*-VCHC-*b*-**2**-*b*-CHC) showed better ductility (ε = 67.4 %) than poly(**4**-*b*-VCHC) and had a σ of 33.0 MPa (entry 6; Figure 6a). These mechanical properties are comparable to those of commodity polyolefins such as polypropylene (σ = 32.4 MPa, ε = 10.2%; entry 7; Figure 6a). Both poly(**4**-*b*-VCHC) and poly(**4**-*b*-VCHC-*b*-**2**-*b*-CHC) had high glass transition temperatures (T_g ≈ 102-103 °C); the values were higher than those of the common polyesters PLA (T_g ≈ 50 °C),[35] poly(ethylene terephthalate) (T_g ≈ 80 °C),[36] and poly(3-hydroxybutyrate) (T_g ≈ 5 °C).[37] The melting temperatures (T_m) were around 165 °C, which is comparable to that of PLA (161 °C) (Table 2, compare entries 5 and 6 with entry 3; Figure S27). Additionally, poly(**4**-*b*-VCHC) exhibited excellent thermal stability, as indicated by thermogravimetric analysis; the degradation temperature at 5% mass loss ($T_{d,5\%}$) was 257 °C (Figure S28).

Next, we prepared toughened elastomers using our functionalized poly(ester-*b*-carbonates). Copolymers comprising elastic (soft) and glassy (hard) blocks usually exhibit characteristics of thermoplastic elastomers,[1a] and this combination is the basis for the commercially successful nondegradable poly(styrene)–poly(diene) copolymers.[38] Because the brittleness of aliphatic polycarbonates such as poly(CHC) and poly(VCHC) has hampered their utility, we hypothesized that including ductile and soft blocks such as poly(**2**) (Table 2, entry 8) would afford a strong, ductile copolymer. Indeed, poly(**2**-*b*-CHC) (74.0 kDa) displayed a σ of 21.4 MPa and an ε of 376.7%, and poly(**2**-*b*-VCHC) (204.2 kDa) was even stronger and more ductile, with a σ of 25.0 MPa and an ε of 406.8% (Figure 6b; Table 2, entries 9 and 10). The addition of the soft poly(**3**) to poly(CHC) and poly(VCHC) also improved ductility, giving copolymers with ε values of 255.2% and 293.0%, respectively, and σ values of less than 20 MPa (Table S6, entries 7 and 11). The modulus of toughness and ductility values of both poly(**2**-*b*-CHC) and poly(**2**-*b*-VCHC) were markedly better than those of LDPE (Figure 6c; comparing entries 9 and 10 with entry 11 in Table 2) and our previously reported polyesters.[15] In addition, thermogravimetric analysis of poly(**2**-*b*-CHC) and poly(**2**-*b*-VCHC) showed that both copolymers had excellent thermal stabilities, with $T_{d,5\%}$ values of 263 and 288 °C, respectively (Figure S28). Notably, poly(**2**-*b*-CHC) showed a T_g of 29 °C with shape-memory recovery at room temperature (Figures S27 and S29; Table S7, entry 2). In contrast, poly(**2**-*b*-VCHC), which had two T_g values (20 and 101 °C), underwent considerable strain hardening with visible white striations, resulting in unrecoverable plastic deformation (Figure S29; Table S7, entry 5).

CONCLUSIONS

Constructing sequence-controlled block copolymers from a mixture of co-monomers has been a long-standing challenge in polymer chemistry. A simple and high-performance synthetic solution to this challenge has been presented herein with obvious advantages in terms of sustainability and ease of scale-up, and having

unique reaction kinetics that enables the perfectly clean switching of the polymerization mechanism during chain propagation. To our knowledge, the scalable synthesis of such high-MW functionalized poly(ester-*b*-carbonates) copolymers from equimolar mixtures of OCAs and epoxides using a single metal complex has never been achieved before. Our method provides access to new degradable materials with a wide range of thermal and mechanical properties comparable to those of currently available nondegradable commodity polyolefins. Although many epoxides are currently produced from nonrenewable resources, epoxides could potentially be synthesized through the metathesis of plant oils followed by epoxidation.[39]

Table 2. Thermal and Mechanical Properties of Various Poly(ester-*b*-carbonates), LDPE, PP, and Corresponding Homopolymers. [a]

Entry	Polymer	M_n (kDa) [b]	$Đ$ [b]	T_g / T_m (°C) [c]	E_y (MPa) [d]	σ (MPa) [d]	ε (%) [d]
1	poly(CHC)	42.9	1.06	115 / -	1007.9 ± 222.6	21.3 ± 1.4	4.0 ± 1.3
2	poly(VCHC)	105.8	1.01	113 / -	1489.9 ± 424.9	28.9 ± 2.1	3.1 ± 0.8
3	poly(**4**) (PLA)	247.7	1.04	- / 161	1303.1 ± 306.1	49.3 ± 3.3	11.5 ± 4.4
4	poly(**4**-*b*-CHC)	103.6	1.05	101 / 166	2740.8 ± 617.9	32.5 ± 2.9	2.6 ± 1.1
5	poly(**4**-*b*-VCHC)	404.2	1.03	103 / 167	1550.0 ± 408.0	44.8 ± 1.6	41.2 ± 17.3
6	poly(**4**-*b*-VCHC-*b*-**2**-*b*-CHC)	176.3	1.04	102 / 164	628.8 ± 19.6	33.0 ± 1.1	67.4 ± 8.6
7	PP [e]	-	-	-	1152.6 ± 262.7	32.4 ± 0.3	10.2 ± 1.9
8	poly(**2**)	45.8	1.01	10 / -	2.1 ± 1.1	0.1 ± 0.04	1307.3 ± 7.9
9	poly(**2**-*b*-CHC)	74.0	1.01	29 / -	135.1 ± 38.1	21.4 ± 1.1	376.7 ± 75.3
10	poly(**2**-*b*-VCHC)	204.2	1.01	20, 101 / -	369.8 ± 37.2	25.0 ± 2.2	406.8 ± 27.1
11	LDPE [f]	-	-	-	160.3 ± 55.1	10.0 ± 0.2	311.6 ± 10.9

[a] Abbreviations: M_n, number-average molecular weight; $Đ$, molecular weight distribution; T_g, glass transition temperature; T_m, melting temperature; E_y, Young's modulus; σ, fracture stress; ε, fracture strain; *b*, block; PLA, poly(lactic acid); PP, polypropylene; LDPE, low-density polypropylene. For all mechanical tests, $n = 4$ or 5, and data are presented as means ± standard deviations. [b] Determined by size-exclusion chromatography. [c] Determined by differential scanning calorimetry. See Figure S27. [d] Determined by stress–strain tests. See Figure S26. [e] Commercially available PP film from Braskem prepared by hot pressing. [f] Commercially available films from McMaster-Carr.

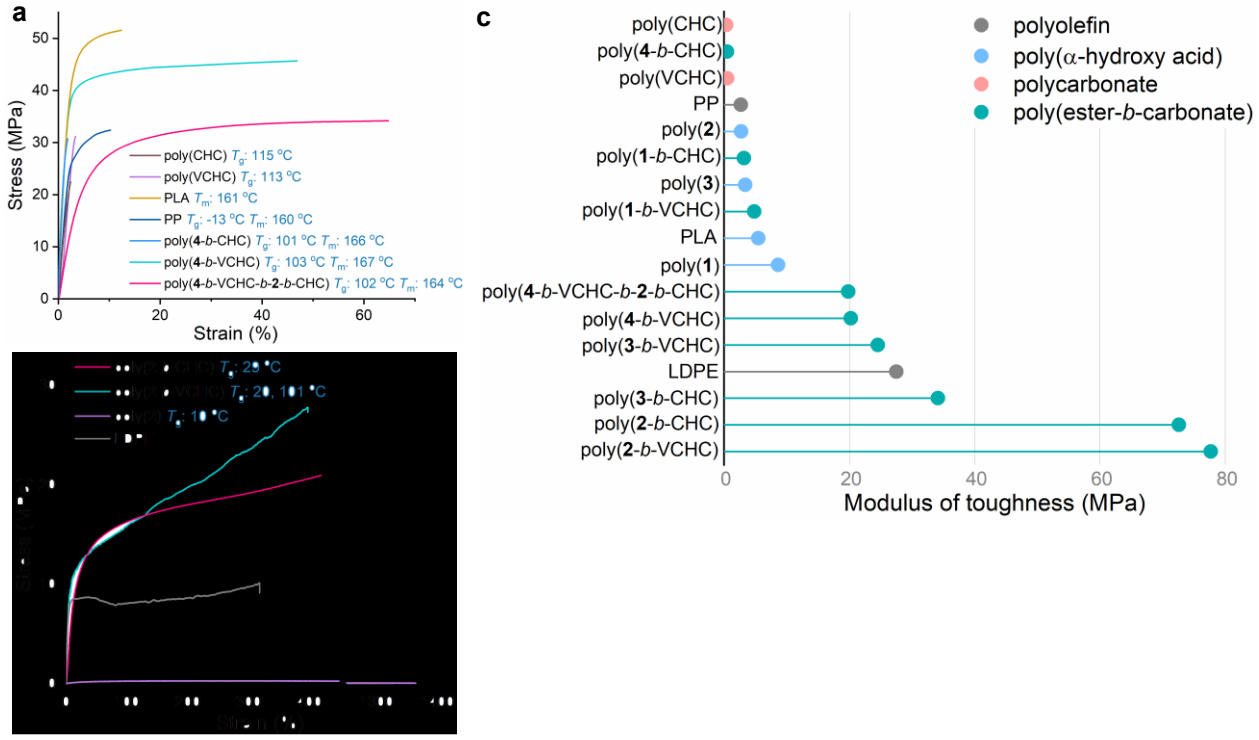

Figure 6. Study of the mechanical properties of strong and tough poly(ester-*b*-carbonates). (a) Representative stress–strain curves obtained by uniaxial extension of various strong poly(ester-*b*-carbonates), their parental homopolymers, and polypropylene (PP). (b) Representative stress–strain curves obtained by uniaxial extension of various ductile and tough poly(ester-*b*-carbonates) and low-density polyethylene (LDPE). (c) Comparison of the modulus of toughness values of various poly(ester-*b*-carbonates) with those of commodity polyolefins, poly(α-hydroxy acids), and polycarbonates. Polymer MWs, *Đ*s, and phase-transition temperatures are provided in Table 2 and Table S6. All stress–strain curves obtained from uniaxial-extension studies are provided in Figure S26.

Mechanistically, four distinctive features in our newly discovered auto-tandem polymerization contribute to this highly efficient chemistry. First, the unique monomer-activation mechanism of OCA with low activation energy barrier ensures the rapid initiation of OCA polymerization. Second, the zero-order kinetics in OCA polymerization significantly suppresses the tapering effect and enables a clean mechanism switch (Figures 2c and 3b). Third, the distinctive ROP mechanism of OCA that involves but does not consume bystander co-monomer allows for a smooth transition to the second polymerization cycle; whereas conventional metal-alkoxide-mediated polymerization could lead to undesired chain termination during the transition (Table S4, entry 5). Fourth, the highly active electron-deficient Zn complex allows for the entire polymerization undergoing at room temperature without pressured gas. As previous attempts that rationalize the distinct mechanism selection behavior by a single catalyst focused on the free energy difference between different polymerization cycles, our findings are important because we reveal such selectivity results both from the low activation barriers and from the beneficial zero-order kinetics at the first stage of the polymerization. The principles described herein provide a new perspective on other polymerization systems concerning sequence control and block resolution.[32b] Exploration of this new chemical space of poly(ester-*b*-carbonates) via stereosequence-controlled synthetic methods[37] would be an imminent step toward improving this promising class of sustainable block copolymers.

ASSOCIATED CONTENT

Supporting Information.

The Supporting Information is available free of charge on the ACS Publications website.

- Detailed experimental procedures; monomers and catalysts synthesis; catalyst screening and reaction optimization; polymerization kinetics and characterization (ESI-MS and MALDI spectroscopy, NMR spectroscopy; SEC); mechanistic considerations and characterization (ESI-MS spectroscopy, infrared spectroscopy) and reaction pathways discussion; thermal and mechanical tests of polymers (DSC, TGA, tensile tests, shape-memory tests).
- Details on the computational methods and computed Cartesian coordinates of structures.

AUTHOR INFORMATION

Corresponding Author

* rtong@vt.edu

Funding Sources

This work was supported by start-up funding from Virginia Tech, ACS-Petroleum Research Foundation (57926-DNI-7), and the National Science Foundation (CHE-1807911).

Notes

The authors declare no competing financial interest.

ACKNOWLEDGMENT

We thank Dr. N. Murthy Shanaiah (Department of Chemistry, Virginia Tech) for NMR spectroscopy experiments, Mehdi Ashraf-Khorassani (Department of Chemistry, Virginia Tech) for electrospray ionization mass spectrometry studies, Dr. Ling Li (Department of Mechanical Engineering, Virginia Tech) and Dr. Thomas Staley (Department of Materials Science and Engineering, Virginia Tech) for mechanical testing, and Dr. Jeffrey Parks (Department of Civil & Environmental Engineering, Virginia Tech) for inductively coupled plasma mass spectrometry measurements, and Dr. Keith Ray (Department of Biochemistry, Virginia Tech) for matrix-assisted laser desorption/ionization mass spectrometry measurements.

REFERENCES

(1) (a) Bates, F. S.; Hillmyer, M. A.; Lodge, T. P.; Bates, C. M.; Delaney, K. T.; Fredrickson, G. H. Multiblock Polymers: Panacea or Pandora's Box? *Science* **2012,** *336,* 434-440. (b) Bates, C. M.; Bates, F. S. 50th Anniversary Perspective: Block Polymers—Pure Potential. *Macromolecules* **2017,** *50,* 3-22.

(2) Lutz, J.-F.; Ouchi, M.; Liu, D. R.; Sawamoto, M. Sequence-Controlled Polymers. *Science* **2013,** *341,* 1238149.

(3) Mecerreyes, D.; Moineau, G.; Dubois, P.; Jérôme, R.; Hedrick, J. L.; Hawker, C. J.; Malmström, E. E.; Trollsas, M. Simultaneous Dual Living Polymerizations: A Novel One-Step Approach to Block and Graft Copolymers. *Angew. Chem. Int. Ed.* **1998,** *37,* 1274-1276.

(4) Bielawski, C. W.; Louie, J.; Grubbs, R. H. Tandem Catalysis: Three Mechanistically Distinct Reactions from a Single Ruthenium Complex. *J. Am. Chem. Soc.* **2000,** *122,* 12872-12873.

(5) (a) Schmidt, S. C.; Hillmyer, M. A. Synthesis and Characterization of Model Polyisoprene−Polylactide Diblock Copolymers. *Macromolecules* **1999,** *32,* 4794-4801. (b) Wu, G.-P.; Darensbourg, D. J.; Lu, X.-B. Tandem Metal-Coordination Copolymerization and Organocatalytic Ring-Opening Polymerization via Water To Synthesize Diblock Copolymers of Styrene Oxide/CO2 and Lactide. *J. Am. Chem. Soc.* **2012,** *134,* 17739-17745.

(6) (a) Jeske, R. C.; Rowley, J. M.; Coates, G. W. Pre-Rate-Determining Selectivity in the Terpolymerization of Epoxides, Cyclic Anhydrides, and CO2: A One-Step Route to Diblock Copolymers. *Angew. Chem. Int. Ed.* **2008,** *47,* 6041-6044. (b) Romain, C.; Williams, C. K. Chemoselective Polymerization Control: From Mixed-Monomer Feedstock to Copolymers. *Angew. Chem. Int. Ed.* **2014,** *53,* 1607-1610. (c) Romain, C.; Zhu, Y.; Dingwall, P.; Paul, S.; Rzepa, H. S.; Buchard, A.; Williams, C. K. Chemoselective Polymerizations from Mixtures of Epoxide, Lactone, Anhydride, and Carbon Dioxide. *J. Am. Chem. Soc.* **2016,** *138,* 4120-4131. (d) Ji, H.-Y.; Wang, B.; Pan, L.; Li, Y.-S. One-Step Access to Sequence-Controlled Block Copolymers by Self-Switchable Organocatalytic Multicomponent Polymerization. *Angew. Chem. Int. Ed.* **2018,** *57,* 16888-16892. (e) Xu, J.; Wang, X.; Hadjichristidis, N. Diblock dialternating terpolymers by one-step/one-pot highly selective organocatalytic multimonomer polymerization. *Nat. Commun.* **2021,** *12,* 7124. (f) Zhang, Z.; Zeng, T.-Y.; Xia, L.; Hong, C.-Y.; Wu, D.-C.; You, Y.-Z. Synthesis of polymers with on-demand sequence structures via dually switchable and interconvertible polymerizations. *Nat. Commun.* **2018,** *9,* 2577.

(7) Kernbichl, S.; Reiter, M.; Adams, F.; Vagin, S.; Rieger, B. CO2-Controlled One-Pot Synthesis of AB, ABA Block, and Statistical Terpolymers from β-Butyrolactone, Epoxides, and CO2. *J. Am. Chem. Soc.* **2017,** *139,* 6787-6790.

(8) Wang, X.; Thevenon, A.; Brosmer, J. L.; Yu, I.; Khan, S. I.; Mehrkhodavandi, P.; Diaconescu, P. L. Redox Control of Group 4 Metal Ring-Opening Polymerization Activity toward l-Lactide and ε-Caprolactone. *J. Am. Chem. Soc.* **2014,** *136,* 11264-11267.

(9) (a) Qi, M.; Dong, Q.; Wang, D.; Byers, J. A. Electrochemically Switchable Ring-Opening Polymerization of Lactide and Cyclohexene Oxide. *J. Am. Chem. Soc.* **2018,** *140,* 5686-5690. (b) Hern, Z. C.; Quan, S. M.; Dai, R.; Lai, A.; Wang, Y.; Liu, C.; Diaconescu, P. L. ABC and ABAB Block Copolymers by Electrochemically Controlled Ring-Opening Polymerization. *J. Am. Chem. Soc.* **2021,** *143,* 19802-19808.

(10) Deacy, A. C.; Gregory, G. L.; Sulley, G. S.; Chen, T. T. D.; Williams, C. K. Sequence Control from Mixtures: Switchable Polymerization Catalysis and Future Materials Applications. *J. Am. Chem. Soc.* **2021,** *143,* 10021-10040.

(11) Sulley, G. S.; Gregory, G. L.; Chen, T. T. D.; Peña Carrodeguas, L.; Trott, G.; Santmarti, A.; Lee, K.-Y.; Terrill, N. J.; Williams, C. K. Switchable Catalysis Improves the Properties of CO2-Derived Polymers: Poly(cyclohexene carbonate-b-ε-decalactone-b-cyclohexene carbonate) Adhesives, Elastomers, and Toughened Plastics. *J. Am. Chem. Soc.* **2020,** *142,* 4367-4378.

(12) (a) Xie, R.; Zhang, Y.-Y.; Yang, G.-W.; Zhu, X.-F.; Li, B.; Wu, G.-P. Record Productivity and Unprecedented Molecular Weight for Ring-Opening Copolymerization of Epoxides and Cyclic Anhydrides Enabled by Organoboron Catalysts. *Angew. Chem. Int. Ed.* **2021,** *60,* 19253-19261. (b) Yang, G.-W.; Zhang, Y.-Y.; Xie, R.; Wu, G.-P. Scalable Bifunctional Organoboron Catalysts for Copolymerization of CO2 and Epoxides with Unprecedented Efficiency. *J. Am. Chem. Soc.* **2020,** *142,* 12245-12255.

(13) (a) Zhang, D.; Boopathi, S. K.; Hadjichristidis, N.; Gnanou, Y.; Feng, X. Metal-Free Alternating Copolymerization of CO2 with Epoxides: Fulfilling "Green" Synthesis and Activity. *J. Am. Chem. Soc.* **2016,** *138,* 11117-11120. (b) Pappuru, S.; Chakraborty, D. Progress in metal-free cooperative catalysis for the ring-opening copolymerization of cyclic anhydrides and epoxides. *European Polymer Journal* **2019,** *121,* 109276. (c) Zhang, J.; Wang, L.; Liu, S.; Kang, X.; Li, Z. A Lewis Pair as Organocatalyst for One-Pot Synthesis of Block Copolymers from a Mixture of Epoxide, Anhydride, and CO2. *Macromolecules* **2021,** *54,* 763-772.

(14) (a) Martin Vaca, B.; Bourissou, D. O-Carboxyanhydrides: Useful Tools for the Preparation of Well-Defined Functionalized Polyesters. *ACS Macro Lett.* **2015,** *4,* 792-798. (b) Yin, Q.; Yin, L.; Wang, H.; Cheng, J. Synthesis and Biomedical Applications of Functional Poly(α-hydroxy acids) via Ring-Opening Polymerization of O-Carboxyanhydrides. *Acc. Chem. Res.* **2015,** *48,* 1777-1787.

(15) Wang, X.; Chin, A. L.; Zhou, J.; Wang, H.; Tong, R. Resilient Poly(α-hydroxy acids) with Improved Strength and Ductility via Scalable Stereosequence-Controlled Polymerization. *J. Am. Chem. Soc.* **2021,** *143,* 16813-16823.

(16) Raman, S. K.; Raja, R.; Arnold, P. L.; Davidson, M. G.; Williams, C. K. Waste not, want not: CO2 (re)cycling into block polymers. *Chemical Communications* **2019,** *55,* 7315-7318.

(17) Tang, J.; Li, M.; Wang, X.; Tao, Y. Switchable Polymerization Organocatalysis: From Monomer Mixtures to Block Copolymers. *Angew. Chem. Int. Ed.* **2022,** *n/a,* e202115465.

(18) Chamberlain, B. M.; Cheng, M.; Moore, D. R.; Ovitt, T. M.; Lobkovsky, E. B.; Coates, G. W. Polymerization of lactide with zinc and magnesium β-diiminate complexes: stereocontrol and mechanism. *J. Am. Chem. Soc.* **2001,** *123,* 3229-3238.

(19) Wang, R.; Zhang, J.; Yin, Q.; Xu, Y.; Cheng, J.; Tong, R. Controlled Ring-Opening Polymerization of O-Carboxyanhydrides Using a β-Diiminate Zinc Catalyst. *Angew. Chem. Int. Ed.* **2016,** *55,* 13010-13014.

(20) Cheng, M.; Moore, D. R.; Reczek, J. J.; Chamberlain, B. M.; Lobkovsky, E. B.; Coates, G. W. Single-Site β-Diiminate Zinc Catalysts for the Alternating Copolymerization of CO2 and Epoxides: Catalyst Synthesis and Unprecedented Polymerization Activity. *J. Am. Chem. Soc.* **2001,** *123,* 8738-8749.

(21) Jeske, R. C.; DiCiccio, A. M.; Coates, G. W. Alternating Copolymerization of Epoxides and Cyclic Anhydrides: An Improved Route to Aliphatic Polyesters. *J. Am. Chem. Soc.* **2007,** *129,* 11330-11331.

(22) Coates, G. W.; Moore, D. R. Discrete Metal-Based Catalysts for the Copolymerization of CO2 and Epoxides: Discovery, Reactivity, Optimization, and Mechanism. *Angew. Chem. Int. Ed.* **2004,** *43,* 6618-6639.

(23) (a) DiCiccio, A. M.; Longo, J. M.; Rodríguez-Calero, G. G.; Coates, G. W. Development of Highly Active and Regioselective Catalysts

for the Copolymerization of Epoxides with Cyclic Anhydrides: An Unanticipated Effect of Electronic Variation. *J. Am. Chem. Soc.* **2016,** *138,* 7107-7113. (b) Reiter, M.; Vagin, S.; Kronast, A.; Jandl, C.; Rieger, B. A Lewis acid β-diiminato-zinc-complex as all-rounder for co- and terpolymerisation of various epoxides with carbon dioxide. *Chem. Sci.* **2017,** *8,* 1876-1882.

(24) Kronast, A.; Reiter, M.; Altenbuchner, P. T.; Jandl, C.; Pöthig, A.; Rieger, B. Electron-Deficient β-Diiminato-Zinc-Ethyl Complexes: Synthesis, Structure, and Reactivity in Ring-Opening Polymerization of Lactones. *Organometallics* **2016,** *35,* 681-685.

(25) Bratsch, S. G. A group electronegativity method with Pauling units. *Journal of Chemical Education* **1985,** *62,* 101.

(26) Nakano, K.; Nozaki, K.; Hiyama, T. Spectral Assignment of Poly[cyclohexene oxide-alt-carbon dioxide]. *Macromolecules* **2001,** *34,* 6325-6332.

(27) Webster, O. W. Living Polymerization Methods. *Science* **1991,** *251,* 887-893.

(28) Paul, S.; Zhu, Y.; Romain, C.; Brooks, R.; Saini, P. K.; Williams, C. K. Ring-opening copolymerization (ROCOP): synthesis and properties of polyesters and polycarbonates. *Chemical Communications* **2015,** *51,* 6459-6479.

(29) Kissling, S.; Lehenmeier, M. W.; Altenbuchner, P. T.; Kronast, A.; Reiter, M.; Deglmann, P.; Seemann, U. B.; Rieger, B. Dinuclear zinc catalysts with unprecedented activities for the copolymerization of cyclohexene oxide and CO2. *Chemical Communications* **2015,** *51,* 4579-4582.

(30) Moore, D. R.; Cheng, M.; Lobkovsky, E. B.; Coates, G. W. Mechanism of the Alternating Copolymerization of Epoxides and CO2 Using β-Diiminate Zinc Catalysts: Evidence for a Bimetallic Epoxide Enchainment. *J. Am. Chem. Soc.* **2003,** *125,* 11911-11924.

(31) Stößer, T.; Sulley, G. S.; Gregory, G. L.; Williams, C. K. Easy access to oxygenated block polymers via switchable catalysis. *Nat. Commun.* **2019,** *10,* 2668.

(32) (a) McGraw, M. L.; Clarke, R. W.; Chen, E. Y. X. Synchronous Control of Chain Length/Sequence/Topology for Precision Synthesis of Cyclic Block Copolymers from Monomer Mixtures. *J. Am. Chem. Soc.* **2021,** *143,* 3318-3322. (b) McGraw, M. L.; Clarke, R. W.; Chen, E. Y. X. Compounded Sequence Control in Polymerization of One-Pot Mixtures of Highly Reactive Acrylates by Differentiating Lewis Pairs. *J. Am. Chem. Soc.* **2020,** *142,* 5969-5973.

(33) Walsh, D. J.; Lau, S. H.; Hyatt, M. G.; Guironnet, D. Kinetic Study of Living Ring-Opening Metathesis Polymerization with Third-Generation Grubbs Catalysts. *J. Am. Chem. Soc.* **2017,** *139,* 13644-13647.

(34) (a) Darensbourg, D. J.; Wei, S.-H. Depolymerization of Polycarbonates Derived from Carbon Dioxide and Epoxides to Provide Cyclic Carbonates. A Kinetic Study. *Macromolecules* **2012,** *45,* 5916-5922. (b) Li, C.; Sablong, R. J.; van Benthem, R. A. T. M.; Koning, C. E. Unique Base-Initiated Depolymerization of Limonene-Derived Polycarbonates. *ACS Macro Lett.* **2017,** *6,* 684-688. (c) Carrodeguas, L. P.; Chen, T. T. D.; Gregory, G. L.; Sulley, G. S.; Williams, C. K. High elasticity, chemically recyclable, thermoplastics from bio-based monomers: carbon dioxide, limonene oxide and ε-decalactone. *Green Chem.* **2020,** *22,* 8298-8307. (d) Singer, F. N.; Deacy, A. C.; McGuire, T. M.; Williams, C. K.; Buchard, A. Chemical Recycling of Poly(Cyclohexene Carbonate) Using a Di-MgII Catalyst. *Angew. Chem. Int. Ed.* **2022,** *61,* e202201785. (e) Yu, Y.; Fang, L.-M.; Liu, Y.; Lu, X.-B. Chemical Synthesis of CO2-Based Polymers with Enhanced Thermal Stability and Unexpected Recyclability from Biosourced Monomers. *ACS Catal.* **2021,** *11,* 8349-8357.

(35) Ovitt, T. M.; Coates, G. W. Stereochemistry of Lactide Polymerization with Chiral Catalysts: New Opportunities for Stereocontrol Using Polymer Exchange Mechanisms. *J. Am. Chem. Soc.* **2002,** *124,* 1316-1326.

(36) Paszkiewicz, S.; Szymczyk, A.; Pawlikowska, D.; Irska, I.; Taraghi, I.; Pilawka, R.; Gu, J.; Li, X.; Tu, Y.; Piesowicz, E. Synthesis and characterization of poly(ethylene terephthalate-co-1,4-cyclohexanedimethylene terephtlatate)-block-poly(tetramethylene oxide) copolymers. *RSC Advances* **2017,** *7,* 41745-41754.

(37) Tang, X.; Westlie, A. H.; Watson, E. M.; Chen, E. Y.-X. Stereosequenced crystalline polyhydroxyalkanoates from diastereomeric monomer mixtures. *Science* **2019,** *366,* 754-758.

(38) Handlin Jr., D. L.; Trenor, S.; Wright, K. Applications of Thermoplastic Elastomers Based on Styrenic Block Copolymers. In *Macromolecular Engineering,* Matyjaszewski K.; Gnanou Y.; and Leibler L., Eds; Wiley: Weinheim, **2007**, 2001-2031.

(39) (a) Winkler, M.; Romain, C.; Meier, M. A. R.; Williams, C. K. Renewable polycarbonates and polyesters from 1,4-cyclohexadiene. *Green Chem.* **2015,** *17,* 300-306. (b) Mathers, R. T.; Shreve, M. J.; Meyler, E.; Damodaran, K.; Iwig, D. F.; Kelley, D. J. Synthesis and Polymerization of Renewable 1,3-Cyclohexadiene Using Metathesis, Isomerization, and Cascade Reactions with Late-metal Catalysts. *Macromolecular Rapid Communications* **2011,** *32,* 1338-1342.

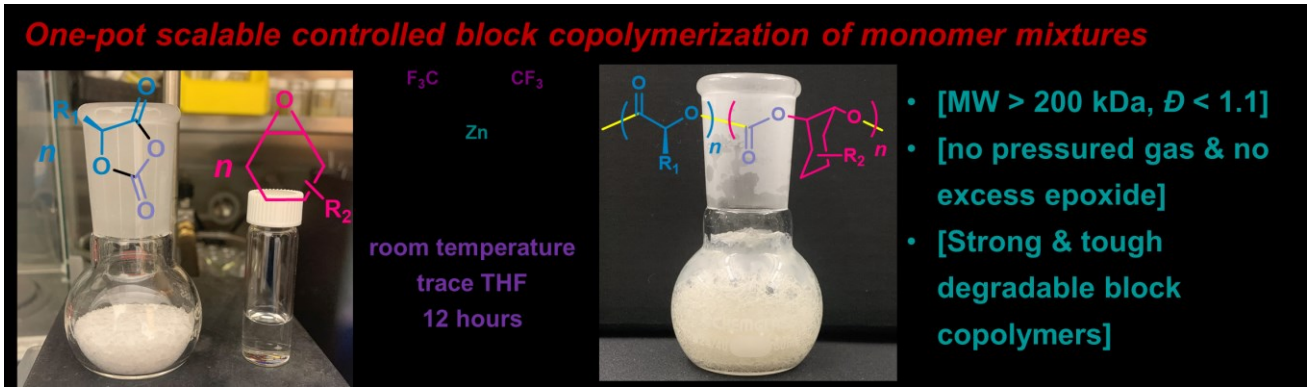
One-pot scalable controlled block copolymerization of monomer mixtures
F3C
CF3
Zn
room temperature
trace THF
12 hours
• [MW > 200 kDa, Đ < 1.1]
• [no pressured gas & no excess epoxide]
• [Strong & tough degradable block copolymers]